



Cite this: *Chem. Commun.*, 2015, 51, 3671

Received 27th December 2014,
Accepted 27th January 2015

DOI: 10.1039/c4cc10351c

www.rsc.org/chemcomm

Charge density mismatch synthesis of MEI- and BPH-type zeolites in the TEA⁺–TMA⁺–Li⁺–Sr²⁺ mixed-structure-directing agent system†

Min Bum Park,‡§ Sang Hyun Ahn,‡ Nak Ho Ahn and Suk Bong Hong*

Nanocrystalline MEI- and BPH-type zeolites, denoted as PST-11 and PST-12, respectively, have been synthesized using both tetraethylammonium and tetramethylammonium ions, the two simplest alkylammonium species, in the presence of Li⁺ and Sr²⁺. PST-12 formation is the first example of a combination of forced and multiple cooperative structure-directions in the charge density mismatch synthesis of zeolites.

Zeolites and related microporous solids, with crystallographically well-defined channels and cavities of molecular dimensions, are not only extending their commercial uses as catalysts and separation media, but also finding new applications, for instance, as insulators in microelectronics.¹ Hence, the synthesis of zeolites with novel framework structures and/or compositions has been a matter of considerable technological interest, as well as of scientific relevance.²

ZSM-18 (IZA code MEI) is unusual in that it is the first zeolite containing 3-rings.³ A rigid aromatic triquatery cation 2,3,4,5,6,7,8,9-octahydro-2,2,5,5,8,8-hexamethyl-1*H*-benzo[1,2-*c*:3,4-*c'*:5,6-*c''*]tripyrrolium (Fig. S1, ESI†) is the organic additive initially used to crystallize this one-dimensional large-pore zeolite in the presence of Na⁺. Because there is a large geometric correspondence between the ZSM-18 cage and the organic guest molecule, ZSM-18 synthesis has been rated as the sole case of true templating in zeolite synthesis. However, quite flexible aliphatic cations, *i.e.*, tris(2-trimethylammonioethyl)amine and triethanolmethylammonium, were subsequently found to direct the synthesis of ZSM-18 and its silicoaluminophosphate analog (ECR-40), respectively.⁴ Moreover, a much simpler but still

asymmetric monoquatery cation choline has been successfully used to synthesize UZM-22, an MEI-type zeolite with a lower Si/Al ratio (*ca.* 5 *vs.* 7), *via* the so-called charge density mismatch (CDM) approach, in which Li⁺ and Sr²⁺ were introduced as crystallization structure-directing agents (SDAs).⁵

We have recently investigated the CDM synthesis of zeolites using tetraethylammonium (TEA⁺) and tetramethylammonium (TMA⁺), the two most studied symmetric organic SDAs, together with Na⁺, to better understand the cooperation between multiple SDAs.⁶ Here we report the synthesis of an MEI-type zeolite with an even lower Si/Al ratio of 3.4, denoted as PST-11, at 120 °C in the TEA⁺–TMA⁺–Li⁺–Sr²⁺ mixed-SDA system. At a higher temperature (*e.g.*, 160 °C), in addition, we were able to crystallize PST-12, a high-silica (Si/Al = 2.6 *vs.* 1.8) version of UZM-4, a BPH-type zeolite synthesized *via* the CDM approach, from the same synthesis mixture. UZM-4 was synthesized initially and subsequently as excellent examples of forced and multiple cooperative structure-directions in TEA⁺–TMA⁺–Li⁺ and choline–Li⁺–(Sr²⁺) mixed-SDA systems, respectively.^{5a,7,8}

In a typical synthesis of PST-11 and PST-12, a clear aluminosilicate solution with the chemical composition 4.0TEAOH·1.0TMACl·0.075LiCl·0.15Sr(NO₃)₂·0.5Al₂O₃·2.5SiO₂·100H₂O was charged into Teflon-lined 45 mL autoclaves and then heated under rotation (60 rpm) at 120 and 160 °C for 6 days, respectively. The phase purity and crystallite size of both zeolites were found to be quite sensitive to the relative concentration of crystallization SDAs (*i.e.*, TMA⁺, Li⁺ and Sr²⁺) in the synthesis mixture, as well as its Si/Al ratio. Further details of their synthesis from a CDM point of view will be given elsewhere.

While the powder X-ray diffraction (XRD) patterns of PST-11 and PST-12 prepared here agree well with those of UZM-22 and UZM-4, respectively, both of them, especially PST-12, are nanocrystalline in nature (Fig. 1). The chemical composition data in Table 1 reveal that despite the considerably higher concentration (TEA⁺/TMA⁺ = 4.0) of TEA⁺ in their synthesis mixture, the crystallization SDA TMA⁺ is the major intrazeolitic organic species. Like the case of UZM-4 synthesis in the TEA⁺–TMA⁺–Li⁺ mixed-SDA system,⁸ which is a well-known example of forced

Center for Ordered Nanoporous Materials Synthesis, Department of Chemical Engineering and School of Environmental Science and Engineering, POSTECH, Pohang 790-784, Korea. E-mail: sbhong@postech.ac.kr

† Electronic supplementary information (ESI) available: Details of experimental procedures; powder XRD, N₂ sorption isotherms, elemental analysis and multinuclear MAS NMR data. See DOI: 10.1039/c4cc10351c

‡ These authors contributed equally to this work.

§ Present address: Institute for Chemical and Bioengineering, ETH Zurich, Wolfgang-Pauli-Strasse 10, CH-8093 Zurich, Switzerland.

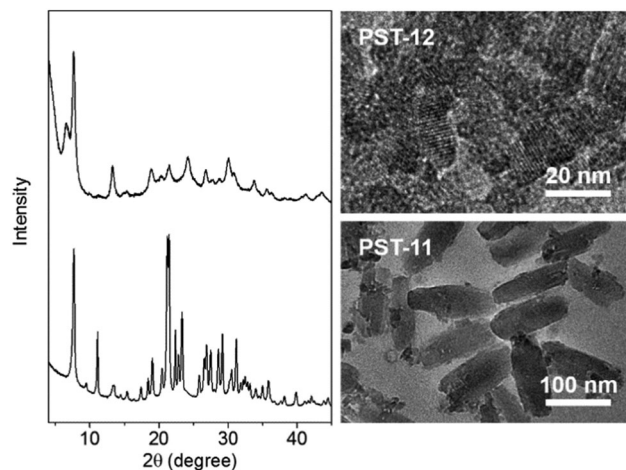


Fig. 1 Powder XRD patterns (left) and TEM images (right) of as-made PST-11 (bottom) and PST-12 (top).

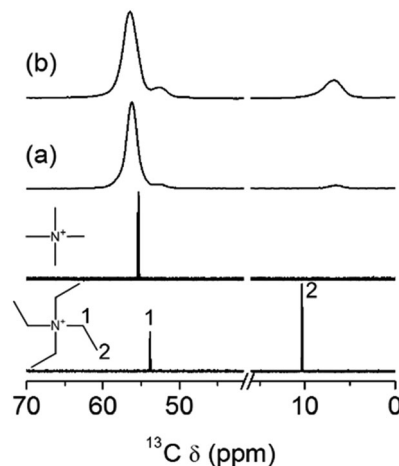


Fig. 2 ^{13}C MAS NMR spectra of as-made (a) PST-11 and (b) PST-12. The solution ^{13}C NMR spectra of TMAcI and TEABr in D_2O (bottom two traces) are also given for comparison.

cooperative structure-direction, in addition, the CDM SDA TEA^+ is hardly incorporated into PST-11. As shown in Table 1, however, a non-negligible amount (1.0 molecule per unit cell) of TEA^+ is present in PST-12, which can be further evidenced using ^{13}C MAS NMR spectroscopy (Fig. 2). We also note that the Si/Al ratio (2.6) of PST-12 is fairly higher than that (1.8) of UZM-4, as supported by ^{29}Si MAS NMR experiments (Fig. S2, ESI †), which may be associated with a notable difference in the content of their TMA^+ and Li^+ ions. To our knowledge, therefore, PST-12 synthesis is the first example where both forced and multiple cooperative structure-directions contribute to zeolite synthesis.

Unlike the case of its high-silica version (*i.e.*, UZM-22), calcination of PST-11 in air at $550\text{ }^\circ\text{C}$ for 8 h to remove the occluded organic species resulted in a serious structural collapse, probably due to its relatively high Al content. This drawback can be overcome by exchanging twice with 1.0 M $\text{NH}_4(\text{NO}_3)$ solutions at $80\text{ }^\circ\text{C}$ for 6 h, leading to a decrease of *ca.* 70 wt% in the organic content, followed by calcination at $550\text{ }^\circ\text{C}$ for 2 h (Fig. S3 and S4, ESI †). While PST-12 has a relatively low Si/Al ratio (2.6 *vs.* 3.4) compared to PST-11, on the other hand, this BPH-type zeolite maintains its structural integrity, to some extent, after calcination at $550\text{ }^\circ\text{C}$ (Fig. S3 and S4, ESI †). Although there is a strong structural resemblance between them, the latter zeolite is less stable than the former one, probably due to the existence of highly strained 3-rings in PST-11. In fact, the lattice energy minimization calculations using the program GULP 9 reveal that the lattice energy per SiO_2 is higher by *ca.* 160 kJ mol^{-1} for the MEI structure than for the BPH one.

Fig. 3 shows the powder XRD patterns of a series of solid products obtained as a function of crystallization time during PST-11 synthesis under rotation (60 rpm) at $120\text{ }^\circ\text{C}$. A broad X-ray peak around $2\theta = 7.7^\circ$ assignable to the (100) reflection of the MEI structure is detectable in the XRD pattern of the solid isolated after 1 day of heating, and crystallization was almost complete after 6 days. Upon prolonged heating, PST-11 was found to be unstable in the crystallization medium, because it becomes transformed into sodalite (SOD). An unexpected result is a small but non-negligible decrease in the solid yield at crystallization times of 4–5 days. This cannot be rationalized without suggesting that PST-11 may grow at the expense of another phase formed at the early period (<4 days) of the crystallization. We also found that the TEA^+/Al and Sr^{2+}/Al ratios of solid products decreases notably when crystallization time is longer than 4 days, whereas the opposite holds for their TMA^+/Al and Si/Al ratios (Fig. S5, ESI †). Since there are no noticeable changes in those ratios with prolonged crystallization time, it is clear that a phase change has occurred between 4 and 5 days.

To more accurately identify the initially formed phase, the X-ray reflections of which are considerably broader than those of fully crystallized PST-11, we obtained the synchrotron powder diffraction pattern of the solid product separated after heating at $120\text{ }^\circ\text{C}$ for 3 days. As shown in Fig. S6 (ESI †), this solid, the Si/Al ratio (2.2) of which is even lower than the ratio of PST-12, is not highly crystalline. However, we were able to notice that the

Table 1 Chemical composition data for zeolites with MEI and BPH topologies

Material	IZA code	Unit cell composition a	Si/Al	Li/Al	Sr/Al	TMA/Al	Ref.
PST-11	MEI	$[\text{TEA}_{0.2}\text{TMA}_{6.1}\text{Li}_{0.5}\text{Sr}_{0.5}(\text{H}_2\text{O})_{14.0}][\text{Al}_{7.8}\text{Si}_{26.2}\text{O}_{68}]$	3.36	0.06	0.06	0.78	This work
UZM-22	MEI	$[\text{Ch}_{5.4}\text{Li}_{0.1}\text{Sr}_{0.3}\text{OH}_{0.2}(\text{H}_2\text{O})_{6.1}][\text{Al}_{5.9}\text{Si}_{28.1}\text{O}_{68}]$	4.76	0.02	0.05	—	6b
PST-12	BPH	$[\text{TEA}_{1.0}\text{TMA}_{5.3}\text{Li}_{0.7}\text{Sr}_{1.3}(\text{H}_2\text{O})_{18.8}][\text{Al}_{9.6}\text{Si}_{24.5}\text{O}_{56}]$	2.55	0.07	0.14	0.55	This work
UZM-4	BPH	$[\text{TEA}_{0.1}\text{TMA}_{3.3}\text{Li}_{6.1}][\text{Al}_{10.0}\text{Si}_{18.0}\text{O}_{56}]$	1.78	0.61	—	0.33	7
		$[\text{Ch}_{4.5}\text{Li}_{1.2}\text{Na}_{1.9}\text{OH}_{0.6}(\text{H}_2\text{O})_{13.1}][\text{Al}_{7.0}\text{Si}_{21.0}\text{O}_{56}]$	2.98	0.17	—	—	This work

a The water content was calculated from the endothermic weight loss by TGA/DTA up to $250\text{ }^\circ\text{C}$. OH^- was introduced to make as-made zeolites electrically neutral.

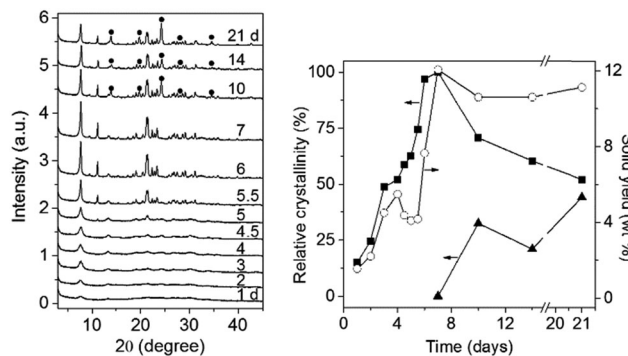


Fig. 3 Powder XRD patterns and relative crystallinities (■) and solid yields (○) for the solid products obtained after PST-11 synthesis at 120 °C for different times. X-ray reflections from sodalite are indicated by closed circles (●), and its relative crystallinities are given by closed triangles (▲). Details on the determination of relative crystallinities of PST-11 and sodalite in each product can be found in the ESI.†

pattern was similar to that of the BPH-type zeolite. Although a small peak around $2\theta = 6.6^\circ$ corresponding to the (001) reflection of the BPH structure is not observable,¹⁰ probably due to the very thin nature of its nanocrystallites perpendicular to the *c*-axis, the positions and relative intensities of all the other reflections match well with those of the X-ray peaks from UZM-4. While the peak around $2\theta = 24.2^\circ$ assignable to the (113) or (212) reflection of the BPH structure, which is missing in the XRD pattern of the MEI structure, is clearly visible, in particular, there are also no detectable peaks around $2\theta = 11.2^\circ$ due to the (002) reflection of the MEI structure.¹⁰ Therefore, it can be concluded that PST-11 formation begins at the rapid expense of BPH-type zeolite nanocrystals of *ca.* 10 nm in length (Fig. S6, ESI†). In fact, quite a similar result was previously reported in the choline-mediated synthesis of UZM-22,^{5a} although no clear evidence for the phase transformation was provided.

It is also remarkable that PST-12 can transform *in situ* into a MEI-type zeolite even at 160 °C, although the transformation rate is considerably slow compared with that at 120 °C (Fig. S7, ESI†). The framework density (14.7), defined as the number of T-atoms per 1000 Å³, of PST-11 with MEI topology is slightly higher than that (14.2) of PST-12 with BPH topology,¹⁰ implying that main driving force for the observed phase transformation is Ostwald ripening through a dissolution/recrystallization. On the other hand, the phase selectivity change caused by increasing the crystallization temperature from 120 to 160 °C cannot be attributed to the lower solubility of the silicate species to form solid products at higher temperature, because the PST-11

sample crystallized at lower temperature has a higher Si/Al ratio than PST-12. Very recently, we have shown that the role of SDAs, especially organic ones, in the CDM synthesis of zeolites varies notably with the crystallization temperature employed,^{6d} which can also be applied to explain the product change described above.

We have successfully synthesized nanocrystalline PST-11 (MEI) and PST-12 (BPH) at 120 and 160 °C, respectively, using the same aluminosilicate solution containing TEA⁺ as a CDM SDA, together with TMA⁺, Li⁺ and Sr²⁺ as crystallization SDAs. The overall characterization results of our work demonstrate that PST-11 and PST-12 syntheses are new examples of forced cooperative structure-direction and of a combination of forced and multiple cooperative structure-directions in the CDM synthesis of zeolites, respectively. The CDM approach is quite useful for directly widening the framework Si/Al ratio range of a particular structure type of zeolites.

This work was supported by the NCRI (2012R1A3A2048833) and BK 21-plus programs through the National Research Foundation of Korea funded by the Korean government (MSIP). We thank J. Cho (POSTECH) for the lattice energy calculations and PAL (Pohang, Korea) for synchrotron diffraction beam time. PAL is supported by MSIP and POSTECH.

Notes and references

- M. E. Davis, *Nature*, 2002, **417**, 813.
- (a) M. E. Davis and R. F. Lobo, *Chem. Mater.*, 1992, **4**, 756; (b) M. A. Cambor and S. B. Hong, in *Porous Materials*, ed. D. W. Bruce, D. O'Hare and R. I. Walton, Wiley, Chichester, U.K., 2011, p. 265.
- S. L. Lawton and W. J. Rohrbaugh, *Science*, 1990, **247**, 1319.
- (a) K. D. Schmitt and G. J. Kennedy, *Zeolites*, 1994, **14**, 635; (b) M. Afeworki, D. L. Dorset, G. J. Kennedy and K. G. Strohmaier, *Stud. Surf. Sci. Catal.*, 2004, **154**, 1274.
- (a) M. A. Miller, J. G. Moscoso, S. C. Koster, M. G. Gatter and G. J. Lewis, *Stud. Surf. Sci. Catal.*, 2007, **170**, 347; (b) M. A. Miller, J. G. Moscoso and G. J. Lewis, *US Pat.*, 7,744,850, 2010; (c) G. Wang, B. Marler, H. Gies, C. A. Fyfe, P. Sidhu, B. Yilmaz and U. Müller, *Microporous Mesoporous Mater.*, 2010, **132**, 43.
- (a) S. H. Kim, M. B. Park, H.-K. Min and S. B. Hong, *Microporous Mesoporous Mater.*, 2009, **123**, 160; (b) M. B. Park, S. J. Cho and S. B. Hong, *J. Am. Chem. Soc.*, 2011, **133**, 1917; (c) M. B. Park, Y. Lee, A. Zheng, F.-S. Xiao, C. P. Nicholas, G. J. Lewis and S. B. Hong, *J. Am. Chem. Soc.*, 2013, **135**, 2248; (d) M. B. Park, D. Jo, H. C. Jeon, C. P. Nicholas, G. J. Lewis and S. B. Hong, *Chem. Mater.*, 2014, **26**, 6684.
- C. S. Blackwell, R. W. Broach, M. G. Gatter, J. S. Holmgren, D.-Y. Jan, G. J. Lewis, B. J. Mezza, T. M. Mezza, M. A. Miller, J. G. Moscoso, R. L. Patton, L. M. Rohde, M. W. Schoonover, W. Sinkler, B. A. Wilson and S. T. Wilson, *Angew. Chem., Int. Ed.*, 2003, **42**, 1737.
- G. J. Lewis, M. A. Miller, J. G. Moscoso, B. A. Wilson, L. M. Knight and S. T. Wilson, *Stud. Surf. Sci. Catal.*, 2004, **154**, 364.
- J. D. Gale and A. L. Rohl, *Mol. Simul.*, 2003, **29**, 291.
- Ch. Baerlocher and L. B. McCusker, Database of Zeolite Structures. <http://www.iza-structure.org/databases/>.